International Journal of Engineering Research & Technology (IJERT)
ISSN: 2278-0181
Vol. 3 Issue 2, February - 2014

White Blood Cell Segmentation using hybrid segmentation methods

Senthilbabu D
Assistant Professor, Department of ECE
Asian College of Engineering and Technology
Coimbatore, India

Maheswari S
Assistant Professor, Department of BME
Sri Ramakrishna Engineering College
Coimbatore, India

***Abstract*—In this paper, the white blood cells identification methods based on the image captured by light microscopy, a microscopy hyper spectral imaging system was used to analyze the blood smears. A hybrid method of snake algorithm and pixel-wise segmentation is proposed to segment the nuclei and cytoplasm of White Blood Cells from the microscopy hyper spectral images. The system was developed by coupling an acousto-optic tunable filter (AOTF) adapter to a microscopy and driven by a SPF Model acousto-optic tunable filter controller, which can capture hyperspectral images. The proposed method is based on the pixel-wise improved spectral angle mapper (ISAM) segmentation, followed by the majority voting within the active contour model regions. Finally, the accuracy of the proposed algorithm is 99.09% (nuclei) and 79.60% (cytoplasm), respectively, because the new method can jointly use both the snake and pixel-wise information of blood cells.**

Keywords—snake algorithm, ISAM and hybrid segmentation

I. INTRODUCTION

The microscopic images blood cell analysis is a powerful diagnostic tool for many types of diseases. There are three major cellular constituents of bloods. They are red cells (Erythrocytes), platelets and white blood cell (leukocytes). White blood cells (WBC) or leukocytes play a significant role in the diagnosis of different diseases, and therefore, extracting information about that is valuable for hematologists. These WBCs can eliminate the gems such as bacteria, viruses, fight cancer cells and other toxic substances[1]. In the past, digital image processing techniques have helped to analyze the cells that lead to more accurate, standard, and remote disease diagnosis systems. However, there are a few complications in extracting the data from WBC due to wide variation of cells in shape, size, edge, and position. Moreover, since illumination is imbalanced, the image contrast between cell boundaries and the background varies depending on the condition during the capturing process.

The most important step of the computer-aided automatic analysis method is blood cell segmentation, which can directly influence the feasibility and reliability of analytical results. In the past decades, researchers have proposed different algorithms to segment the WBCs automatically from the microscopy images of blood smears. Harms proposed a segmentation strategy that characteristic color difference thresholds for each nucleus and cytoplasm combined with geometric operations, probability functions, and cell model [2]. The different kinds of algorithms have been proposed to segment the WBCs such as the active contour models [3], the feature space clustering based algorithm [4], the stepwise merging rules and gradient vector flow snake method [5], the multilevel thresholding [6], and the neural network model [7]. The hyperspectral imaging, also known as imaging spectroscopy or spectral imaging, is a technology that can provide a digital image with far more spectral (color) information for each pixel than traditional color cameras. Different kinds of microscopy hyperspectral imaging system have been developed and used for biomedical analysis of various biological tissues. The microscopy hyperspectral imaging technology can obtain both images (structural information) and spectra (biochemical information) of biological tissues which have the significant advantages in the area of life science.

II. HYPERSPECTRAL IMAGE

The microscopy hyperspectral imaging system used in this paper consists of a microscope, an AOTF adapter, a SPF Model AOTF controller, high-density cooled charge coupled device detector, a data collection and control module and a personal computer. The minimum wavelength selection sweep interval of the AOTF adapter, which makes it possible for the system to capture the microscopy hyperspectral images quickly. The microscopy hyperspectral imaging system can capture hundreds of spectral bands covering the narrow spectral features of the captured blood smears with high accuracy.

As shown in Fig. 1, the microscopy hyperspectral data can be visualized as a three dimensional cube. From the figure it can be seen that the microscopy hyperspectral images of blood smears contain both spectral and spatial in formation of blood cells, which makes it possible to improve the accuracy of the automated WBCs segmentation with some new hyperspectral based algorithms.

III. PRE-PROCESSING TECHNIQUE

The purpose of the pre-processing procedure is to remove unwanted effects (noises) from the image, calibrate the in homogeneous spectral response of the system and transform or adjust the image as necessary for further processing. In the past decades, researchers have proposed several kinds of pre-processing methods for the hyperspectral images. In

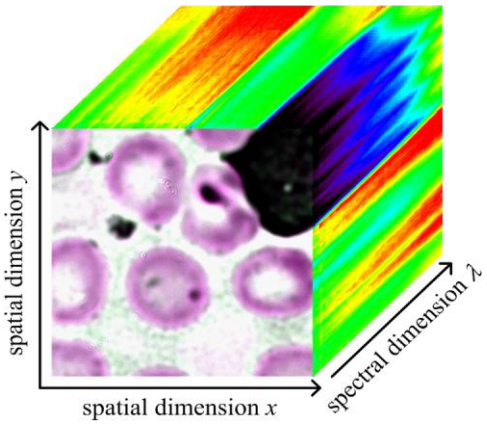

Fig. 1 microscopy hyperspectral data cube.

this study, the expectation maximization approach proposed by Wachman was used to remove the effect of the acoustic angle distribution on the spectral band pass of an AOTF adapter [8].

A calibration method was used to remove the effects of the emission spectra of the illumination sources, the transmission of the optics in microscope, and the detection sensitivity of the CCD camera. In the calibration process, a thin diffusing glass slide with approximately 95% transmittance across the 550nm to 1000nm spectral range is selected as the calibration specimen to capture the calibration data (both the bright and dark images) using identical exposure settings as the blood smears. Then the gray correction coefficient was calculated to calibrate the spectral response of the system for each scene of microscopy hyperspectral images of blood smears. In addition, the microscopy hyperspectral images also need to be normalized to get the transmittance data for further analysis. The calibration and normalization procedure can be performed according to the following equation

$$T(x,y;\lambda) = \frac{log\,(BM_w(x,y;\lambda) - BM_d(x,y;\lambda))}{((BM_b(x,y;\lambda) - BM_d(x,y;\lambda))Tslide)} \qquad (1)$$

where $T(x,y;\lambda)$ denotes the normalized transmittance image of blood smear, $BM_w(x,y;\lambda)$ denotes the intensity values of bright calibration data, BM_d denotes the intensity values of dark calibration data, BM_b denotes the intensity image of blood smears, and T_{slide} denotes the transmittance of the calibration slide specified by the manufacturer. Fig. 3(b) shows the experimental results of the pre-processing images.

IV. SEGMENTATION

A. Principal Component Analysis

One of the properties of this method is the ability to make continuous edges even if the edge is weak or broken, which is very suitable for WBCs segmentation. However, the active contour models can hardly be performed directly on the microscopy hyperspectral data as it generally contains hundreds of single band images. To obtain a one-band image which would contain enough information for active contour models, the principal component analysis (PCA) method is used to map these single band images on to a vector space where an actual ordering relation exists. Principal component analysis (PCA) is a statistical procedure that uses orthogonal transformation to convert a set of observations of possibly correlated variables into a set of values of linearly uncorrelated variables called principal components.

The number of principal components is less than or equal to the number of original variables. This transformation is defined in such a way that the first principal component has the largest possible variance (that is, accounts for as much of the variability in the data as possible), and each succeeding component in turn has the highest variance possible under the constraint that it is orthogonal to (i.e., uncorrelated with) the preceding components. Principal components are guaranteed to be independent if the data set is jointly normally distributed. PCA is sensitive to the relative scaling of the original variables.

B. Snake Algorithm

Active contour model, also called snakes, is a framework for delineating an object outline from a possibly noisy 2D image. This framework attempts to minimize an energy associated to the current contour as a sum of an internal and external energy. The external energy is supposed to be minimal when the snake [9] is at the object boundary position. Nuclei have variable shapes in different kinds of leukocytes. Finding a significant method for shape modelling and segmenting the nucleus has always been a challenge for scientists. Among segmentation methods, active contour models (snakes) have gained a lot of attention recently [26]. Snakes are deformable curves that can move and change their shapes to deform to boundaries of objects in an image. Curves are defined within an image domain and can move under the influence of internal forces within the curve itself and external forces derived from the image data. The internal and external forces are defined in a way that the snake conforms to an object boundary or other desired features within an image [26, 27].

The most straight forward approach consists in giving low values when the regularized gradient around the contour position reaches its peak value. The internal energy is supposed to be minimal when the snake has a shape which is supposed to be relevant considering the shape of the sought object. The most straightforward approach grants high energy to elongated contours (elastic force) and to bended high curvature contours (rigid force), considering the shape should be as regular and smooth as possible.

In Snakes, we use the technique of matching a deformable model to an image by means of energy minimization. A snake initialized near the target gets refined iteratively and is attracted towards the salient contour. A snake in the image can be represented as a set of n points. Fig. 3(c) shows the experimental results of active contour method (Snake). Nuclei have variable shapes in different kinds of leukocytes. Finding a significant method for shape modelling and segmenting the nucleus has always been a challenge for scientists. Among segmentation

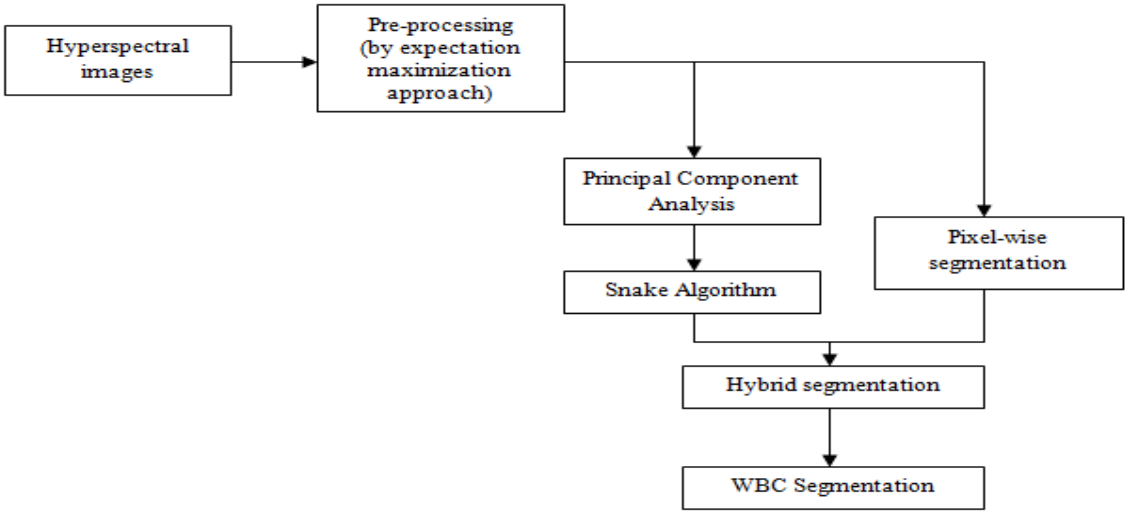

Fig. 2. Flow chart for the proposed method

methods, active contour models (snakes) have gained a lot of attention recently [5]. Snakes are deformable curves that can move and change their shapes to deform to boundaries of objects in an image. Curves are defined within an image domain and can move under the influence of internal forces within the curve itself and external forces derived from the image data. The internal and external forces are defined in a way that the snake conforms to an object boundary or other desired features within an image.

C. *Pixel-wise Segmentation*

To utilize the spectral information of microscopy hyperspectral images for WBCs segmentation, the ISAM algorithm was introduced to the segmentation. The spectral angle mapper (SAM) algorithm is one of the commonly used methods to segment the target from the hyperspectral images in remote sensing field. It was proposed by Kruse et al. To determine the spectral similarity between two spectra by calculating the 'angle' between them [10]. Smaller angle between the test spectrum and the reference spectrum represents closer matches to the target. Therefore, the targets can be segmented from the hyperspectral images with a threshold value of SA.

However, this method often leads to some segment--ation errors when the wavelengths shifting several bands with the influence of noise. To overcome this disadvantage, we use the improved spectral angle mapper (ISAM) algorithm in this paper. The ISAM algorithm calculates the spectral angle (SA) between reference spectrum and the test spectrum with shift forward and backward one or two bands. Fig. 3(d) shows the experimental results of pixel-wise segmentation method.

V. Hybrid Segmentation

By combining the active contour models and the ISAM, we can get the snake algorithm and pixel-wise segmentation to segment the WBCs from the microscopy hyperspectral images of blood smears. Fig. 2 shows the general flow-chart of the proposed segmentation algorithm. At the input we have the microscopy hyperspectral data cube of blood smears. After pre-processing, the PCA transformation is performed on the data and the first principal component is selected for the active contour model analysis. Then, the ISAM is performed on the microscopy per spectral images to segment them into regions. Consequently, this independent candidate segmentations results should be somehow combined into a single final segmentation.

Among all the combination methods, majority vote (also named majority rule, decision fusion or label voting) is by far the simplest for implementation. This method does not need to assume prior knowledge of the behaviour of the individual segmentation, and it also does not require training on large quantities of representative recognition results from the experts [11]. After the active contour models and the ISAM process, we use the majority voting rule to fuse the segmentations by weighting each candidate result equally and assigning to each pixel the label that most segmentation results agree on. Fig. 3(e) shows the experimental results of integrated segmentation method.

VI. WBC Segmentation

By combining the active contour models and the ISAM, we can get the snake and pixel-wise segmentation to segment the WBCs from the micro scopy hyper spectral images of blood smears. Fig. 2 shows the general flow-chart of the proposed segm--entation algorithm. The WBCs can be segmented accurately by using both snake and pixel-wise segmentation contained in the microscopy hyper spectral images.

Fig. 3(c) shows the experimental results of WBC segmentation. In this, we use segmentation the microscopy hyper spectral imaging system to capture the images of blood cells and proposed the snake and pixel-wise segmentation to segment the nuclei and cytoplasm of WBCs. The results for each method were compared with the manually extracted segmentation results (the ground truth) and the error ratio estimated using the following equations [12].

$$N_U = Card(M-(M \cap A))/S_M \qquad (2)$$

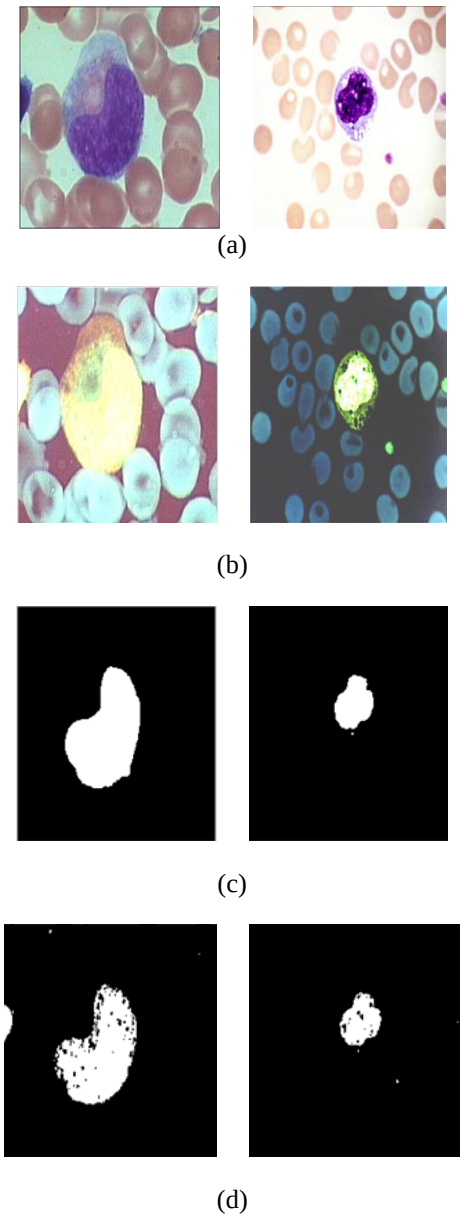

Fig. 3. Experimental Results. (a) Input images (b) Pre-processing images (c) Active contour Segmentation (d) Pixel-wise segmentation (e) Hybrid segmentation (f) WBC segmentation

$$N_O = Card(A-(M \cap A))/S_A \quad (3)$$

$$Avg = (1-(N_U \oplus N_O)) \quad (4)$$

where M denotes the set of pixels in the manually segmented region, A denotes the set of pixels in the automatically extracted region when using the SID algorithm or the proposed algorithm, S_M and S_A represent the total number of pixels in M and A, respectively, N_U and N_O denotes the inaccuracy of the under segmentation ratio and over segmentation ratio, respectively, the symbol $Card(M)$ denotes the cardinality of set M, Avg represents the accuracy between the ground truth and the automated segmented region where a number closer to 1 represents a lower error and higher accuracy, while a number closer to 0 represents a higher error and lower reliability. Table 1 lists the performance evaluation results of the SID and snake and pixel-wise segmentation using Equations (2), (3), (4). From the table. 1 it can be seen that the proposed method has a lower over and under segmentation error ratio and a higher average accuracy.

TABLE 1 COMPARISONS OF PERFORMANCE OF THE SID AND THE PROPOSED ALGORITHMS.

Measure	SID Algorithm				Proposed method			
	Nuclei		Cytoplasm		Nuclei		Cytoplasm	
N_U	10.1523	5.3576	10.5537	16.9476	0.0039	0.0055	2.9182	13.9718
N_O	4.7712	9.8345	12.4611	19.5693	0.0053	0.0036	1.6970	6.4211
Avg	85.0765	84.8079	76.9852	63.4831	99.9909	99.9909	95.3847	79.6071

Therefore, the proposed segmentation method produced a better performance than the comparative algorithm as regards nuclei and cytoplasm. One of the reasons for the good performance of the proposed methods in both N_U and N_O was that false positive regions were effectively removed by using both the snake and pixel-wise information of the microscopy hyper spectral images.

VII. CONCLUSION

A hybrid WBCs identification and segmentation algorithms have been proposed to assist biologists. Most of these methods are based on the color or gray images of blood smears captured by light microscopy and make it pre-processing. Then a snake algorithm and pixel-wise segmentation scheme is proposed for segmenting the nuclei and cytoplasm of WBCs. The new method is based on the pixel-wise ISAM segmentation algorithm, followed by majority voting with in the ACM regions. The proposed method can improve the segmentation performances by the incorporation of the spatial information into the segmentation process. In the future study, we will propose some new algorithms to perform the detailed analysis on the blood smears, such as the classification of different kinds of blood cells, the cell counting, the morphological parameters calculation, and the degree of oxygen saturation retrieval, which may be useful for a better interpretation of further studies involving the structural and biochemical changes and experimental models of diseases.

REFERENCES

[1] Khashman A. IBCIS: "intelligent blood cell identification system".Progress in Natural Science 2008; 18: 1309–14.
[2] Harms H, Aus HM, Haucke M, Gunzer U. "Segmentation of stained blood cell images measured at high scanning density with high magnification and high numerical aperture optics". Cytometry 1986; 7: 522–31.
[3] Yang L, Meer P, Foran DJ. "Unsupervised segmentation based on robust estimation and color active contour models". IEEE Transactions on Information Technology in Biomedicine 2005; 9: 475–86.
[4] Jiang K, Liao QM, Xiong Y. "A novel white blood cell segmentation scheme based on feature space clustering". Soft Computing 2006; 10: 12–9.
[5] Ko BC, Gim J-W, Nam J-Y. "Automatic white blood cell segmentation using stepwise merging rules and gradient vector flow snake". Micron 2011; 42: 695–705.
[6] Adollah R, Mashor MY, Rosline H, Harun NH. "Multilevel thresholding as a simple segmentation technique in acute leukemia images". Journal of Medical Imaging and Health Informatics 2012; 2: 285–8.
[7] Khashman A. "Investigation of different neural models for blood cell type identification". Neural Computing & Applications 2012; 21: 1177–83.
[8] Wachman ES, Niu WH, Farkas DL. "Imaging acousto-optic tunable filter with 0.35-micrometer spatial resolution". Applied Optics 1996 ; 35: 5220–6.
[9] Klemencic A, Kovacic S, Pernus F. "Automated segmentation of muscle fiber images using active contour models". Cytometry 1998; 32: 317–26.
[10] Park J, Keller JM. "Snakes on the watershed". IEEE Transactions on Pattern Analysis and Machine Intelligence 2001; 23: 1201–5.
[11] Lam L, Suen CY. "Application of majority voting to pattern recognition: an analysis of its behavior and performance". IEEE Transactions on Systems Man and Cybernetics, Part A: Systems and Humans 1997; 27: 553–68.
[12] Ko B, Seo M, Nam JY. "Microscopic cell nuclei segmentation based on adaptive attention window". Journal of Digital Imaging 2009; 22: 259–74.
[13] Ceelie H, Dinkelaar RB, van Gelder W. "Examination of peripheral blood films using automated microscopy; evaluation of Diffmaster Octavia and Cellavision DM96". Journal of Clinical Pathology 2007; 60: 72–9.
[14] Guo N, Zeng L, Wu Q. "A method based on multi spectral imaging technique for white blood cell segmentation". Computers in Biology and Medicine 2007; 37: 70–6.
[15] Guan Y, Li Q, Wang Y, Liu H, Zhu Z. Pathological leucocyte segmentation algorithm based on hyper spectral imaging technique. Optical Engineering 2012;51.
[16] Kass M, Witkin A, Terzopoulos D. "Snakes: active contour models". International Journal of Computer Vision 1987; 1: 321–31.
[17] Klemencic A, Kovacic S, Pernus F. "Automated segmentation of muscle fiber images using active contour models". Cytometry 1998; 32: 317–26.
[18] Goetz AFH, Vane G, Solomon JE, Rock BN. "Imaging spectrometry for earth remote sensing". Science 1985; 228: 1147–53.
[19] Morris HR, Hoyt CC, Treado PJ. "Imaging spectrometers for fluorescence and raman microscopy-acousto optic and liquid-crystal tunable filters". Applied Spectroscopy 1994; 48: 857–66.
[20] Shonat RD, Wachman ES, Niu WH, Koretsky AP, Farkas DL. "Near-simultaneous hemoglobin saturation and oxygen tension maps in mouse brain using an AOTF microscope". Biophysical Journal 1997; 73: 1223–31.
[21] Li Q, Wang Y, Zhang J, Xu G, Xue Y. "Quantitative analysis of protective effect of erythropoietin on diabetic retinal cells using molecular hyperspectral imaging technology". IEEE Transactions on Biomedical Engineering 2010; 57: 1699–706.
[22] Uhr JW, Huebschman ML, Frenkel EP, Lane NL, Ashfaq R, Liu HY, Rana DR, Cheng L, Lin AT, Hughes GA, Zhang XJJ, Garner HR. "Molecular profiling of individual tumor cells by hyperspectral micro scopic imaging". Translational Research 2012; 159: 366–75.
[23] Kruse, F.A., Lefkoff, A.B., and Boardman, J.W., "The spectral image processing system (SIPS)-software for integrated analysis of AVIRIS data", presented at the Summaries of the 4th Annual JPL Airborne Geoscience Workshop, Pasadena, 1992.
[24] Ertuerk A, Ertuerk S. "Unsupervised segmentation of hyperspectral images using modified phase correlation". IEEE Geoscience and Remote Sensing Letters 2006; 3: 527–31
[25] De La Vega SH, Manian V. "Object segmentation in hyperspectral images using active contours and graph cuts". International Journal of Remote Sensing 2012; 33: 1246–63.
[26] Kass M, Witkin A, Terzopoulos D. "Snakes: active contour models". Comput Graph Image Process. 1988; 1: 321–331.
[27] Xu C, Prince JL. "Snakes, shapes, and gradient vector flow". IEEE Trans Image Process 1998; 7: 359–369.
[28] Khashman A. "Investigation of different neural models for blood cell type identification". Neural Computing & Applications 2012; 21: 1177–83.
[29] Goetz AFH, Vane G, Solomon JE, Rock BN. "Imaging spectrometry for earth remote sensing". Science 1985; 228: 1147–53.